

Data Fusion for System Identification of the Humber Bridge

Michael Döhler, Bijaya Jaishi, Laurent Mevel, and James M.W. Brownjohn

Abstract In Operational Modal Analysis (OMA) of large structures, ambient vibration data from multiple non-simultaneously recorded measurement setups is often needed to be processed. These setups share some sensors in common, while the others are moved from one setup to the next. Like this detailed mode shapes of the structure can be obtained, mimicking lots of sensors, while in fact only a few sensors are used for the measurements. Recently, the “Pre Global Estimation Re-Scaling” (PreGER) for the Stochastic Subspace Identification (SSI) was proposed to obtain global modal parameters of the structure. It is a fully automated method that takes differences in the unmeasured background excitation levels between the setups into account, merges the data and does the global system identification. Like this, the different measurement setups can be processed in one step and do not have to be analyzed separately. In this paper, system identification results of the Humber bridge are presented, which is a challenging example as a big number of setups is available and special measures need to be taken to avoid numerical explosion of the computation. The results are compared to the PoSER approach (Post Separate Estimation Re-Scaling) with data-driven SSI.

1 Introduction

Subspace-based linear system identification methods have been proven efficient for the identification of the eigenstructure of a linear multivariable system in many applications. In this paper, the main motivation is output-only structural identification

Michael Döhler, Laurent Mevel

INRIA, Centre Rennes - Bretagne Atlantique, Campus de Beaulieu, F-35042 Rennes, France, e-mail: michael.doehler@inria.fr, laurent.mevel@inria.fr

Bijaya Jaishi, James M.W. Brownjohn

Department of Civil & Structural Engineering, University of Sheffield, Sir Frederick Mappin Building, Sheffield S1 3JD, UK, e-mail: b.jaishi@sheffield.ac.uk, j.brownjohn@sheffield.ac.uk

in vibration mechanics, of a structure subject to ambient unmeasured vibrations, by using accelerometer measurements or strain gauges, when several successive data sets are recorded, with sensors at different locations in the structure. For doing this, some of the sensors, called the *reference sensors*, are kept fixed, while the others are moved. Like this, we mimic a situation in which lots of sensors are available, while in fact only a few are at hand.

However, there is one unpleasant feature of structural identification of structures subject to ambient excitation, namely that excitation is typically turbulent in nature and nonstationary. Like this, the excitation level can change from setup to setup, which has to be taken into account when merging the sensor data for structural identification.

Two merging strategies are considered that differ in the order of the normalization, identification and merging step: the classical PoSER approach and the previously presented PreGER approach in [6, 8]. Special care is taken of the PreGER approach, which is improved to be able to handle a large number of measurement setups without running into memory problems. The PoSER and the now modular PreGER approach are tested and compared on data measured on the Humber bridge in England using 26 different measurement setups with the data-driven SSI algorithm UPC [12, 11].

2 Stochastic Subspace Identification (SSI)

2.1 Single Setup

2.1.1 State Space Model

We consider a linear multi-variable output-only system described by a discrete-time state space model

$$\begin{cases} X_{k+1} &= F X_k + V_{k+1} \\ Y_k^{(\text{ref})} &= H^{(\text{ref})} X_k \\ Y_k^{(\text{mov})} &= H^{(\text{mov})} X_k \end{cases} \quad (1)$$

with

- X_k the state vector at time instant k ,
- $Y_k^{(\text{ref})}$ the observed output vector of the reference sensors (which are a subset of all sensors),
- $Y_k^{(\text{mov})}$ the observed output vector of all the sensors minus the reference sensors (the remaining sensors),
- $H^{(\text{ref})}$ the observation matrix with respect to the reference sensors,
- $H^{(\text{mov})}$ the observation matrix with respect to the remaining sensors,
- F the state transition matrix,
- V_k the unmeasured stationary Gaussian white noise.

Let furthermore

- $Y_k = \begin{pmatrix} Y_k^{(\text{ref})} \\ Y_k^{(\text{mov})} \end{pmatrix}$ all the observed output at time instant k ,
- $H = \begin{pmatrix} H^{(\text{ref})} \\ H^{(\text{mov})} \end{pmatrix}$ the full observation matrix,
- N the number of measurements ($k = 1, \dots, N$),
- r the total number of sensors and $r^{(\text{ref})}$ the number of reference sensors.

2.1.2 SSI with Unweighted Principal Component (UPC) Algorithm

The classical reference-based data-driven subspace identification of the eigenstructure (λ, ϕ_λ) of the system (1) consists of the following steps for the Unweighted Principal Component algorithm [11, 12]: The parameters p and q are chosen, normally as $p + 1 = q$ as recommended in [1]. Then, the data matrices

$$\mathcal{Y}_{p+1}^+ \stackrel{\text{def}}{=} \begin{pmatrix} Y_{q+1} & Y_{q+2} & \vdots & Y_{N-p} \\ Y_{q+2} & Y_{q+3} & \vdots & Y_{N-p+1} \\ \vdots & \vdots & \vdots & \vdots \\ Y_{q+p+1} & Y_{q+p+2} & \vdots & Y_N \end{pmatrix}, \quad \text{and} \quad \mathcal{Y}_q^- \stackrel{\text{def}}{=} \begin{pmatrix} Y_q^{(\text{ref})} & Y_{q+1}^{(\text{ref})} & \vdots & Y_{N-p-1}^{(\text{ref})} \\ Y_{q-1}^{(\text{ref})} & Y_q^{(\text{ref})} & \vdots & Y_{N-p-2}^{(\text{ref})} \\ \vdots & \vdots & \vdots & \vdots \\ Y_1^{(\text{ref})} & Y_2^{(\text{ref})} & \vdots & Y_{N-p-q}^{(\text{ref})} \end{pmatrix} \quad (2)$$

are built and the “subspace matrix”¹

$$\mathcal{H}_{p+1,q} = \mathcal{Y}_{p+1}^+ \mathcal{Y}_q^{-T} \left(\mathcal{Y}_q^- \mathcal{Y}_q^{-T} \right)^{-1} \mathcal{Y}_q^- \quad (3)$$

is computed. With the factorization $\mathcal{H}_{p+1,q} = \mathcal{O}_{p+1} \mathcal{X}_q$ into matrix of observability and Kalman filter state sequence with

$$\mathcal{O}_{p+1} \stackrel{\text{def}}{=} \begin{pmatrix} H \\ HF \\ HF^2 \\ \vdots \\ HF^p \end{pmatrix} \quad (4)$$

the matrices H as the first block row of \mathcal{O}_{p+1} and F from the least squares solution of

¹ As $\mathcal{H}_{p+1,q}$ is usually a very big matrix and difficult to handle, we continue the calculation in practice with the R part from an RQ-decomposition of the data matrices, see [11] for details. This will lead to the same results as only the left part of the decomposition of $\mathcal{H}_{p+1,q}$ is needed.

$$\begin{pmatrix} H \\ HF \\ \vdots \\ HF^{p-1} \end{pmatrix} F = \begin{pmatrix} HF \\ HF^2 \\ \vdots \\ HF^p \end{pmatrix}$$

are retrieved. Finally, the eigenstructure (λ, ϕ_λ) of the system (1) is obtained from

$$\det(F - \lambda I) = 0, \quad F \phi_\lambda = \lambda \phi_\lambda, \quad \phi_\lambda = H \phi_\lambda.$$

In the following, the subscripts of the matrices $\mathcal{H}_{p+1,q}$, \mathcal{Y}_{p+1}^+ , \mathcal{Y}_q^- and \mathcal{O}_{p+1} are skipped for simplicity.

2.2 Multiple Setups

Instead of a single record for the output (Y_k) of the system (1), N_s records

$$\underbrace{\begin{pmatrix} Y_k^{(1,\text{ref})} \\ Y_k^{(1,\text{mov})} \end{pmatrix}}_{\text{Record 1}} \underbrace{\begin{pmatrix} Y_k^{(2,\text{ref})} \\ Y_k^{(2,\text{mov})} \end{pmatrix}}_{\text{Record 2}} \cdots \underbrace{\begin{pmatrix} Y_k^{(N_s,\text{ref})} \\ Y_k^{(N_s,\text{mov})} \end{pmatrix}}_{\text{Record } N_s} \quad (5)$$

are now available collected successively. Each record j contains data $Y_k^{(j,\text{ref})}$ from a fixed *reference* sensor pool, and data $Y_k^{(j,\text{mov})}$ from a *moving* sensor pool. To each record $j = 1, \dots, N_s$ corresponds a state-space realization in the form

$$\begin{cases} X_{k+1}^{(j)} &= F X_k^{(j)} + V_{k+1}^{(j)} \\ Y_k^{(j,\text{ref})} &= H^{(\text{ref})} X_k^{(j)} \quad (\text{reference pool}) \\ Y_k^{(j,\text{mov})} &= H^{(j,\text{mov})} X_k^{(j)} \quad (\text{sensor pool } n^o j) \end{cases} \quad (6)$$

with a single state transition matrix F .

Note that the unmeasured excitation $V^{(j)}$ can be different for each setup j as the environmental conditions can slightly change between the measurements. However, during each setup j the noise $V^{(j)}$ is assumed to be stationary. Note also that the observation matrix $H^{(\text{ref})}$ is independent of the specific measurement setup if the reference sensors are the same throughout all measurements $j = 1, \dots, N_s$.

For each setup j we obtain a “local” subspace matrix

$$\mathcal{H}^{(j)} = \mathcal{Y}_{(j)}^+ \mathcal{Y}_{(j)}^{-T} \left(\mathcal{Y}_{(j)}^- \mathcal{Y}_{(j)}^{-T} \right)^{-1} \mathcal{Y}_{(j)}^- \quad (7)$$

according to equations (2)-(3), where $\mathcal{Y}_{(j)}^+$ is filled with data from all the sensors and $\mathcal{Y}_{(j)}^-$ with data from the reference sensors of this setup (see Equation (2)). The question is now how to adapt the subspace identification from Section 2.1 to

- merge the data from the multiple setups $j = 1, \dots, N_s$ to obtain global modal parameters (natural frequencies, damping ratios, mode shapes), and to
- normalize or re-scale the data from the multiple setups as the background excitation may differ from setup to setup.

In the following section we present two approaches for this problem: the common practice approach PoSER that processes all the setups separately and merges them at the end, and the recently generalized approach PreGER, that processes all the setups together.

3 Merging Strategies

3.1 Post Separate Estimation Re-Scaling (PoSER)

In this work, reference based SSI-DATA algorithm [12] is used for system identification as PoSER approach. It involves two main steps; processing and modal parameter identification of each setup separately and then merging the modal data. The first step consists of (i) assembly of and QR factorization of data block Hankel matrix (ii) SVD of projection matrix (iii) calculation of system matrices (iv) computation of modal parameters. In the second step, the modal data from each setup are merged to get the global values of system. The values of all setups are averaged to get the natural frequencies and damping ratios of whole structure.

Every setup of simultaneously measured channels yields after identification a part of the global mode shape. These parts are glued together with the aid of the reference sensors, common to all setups. Least squares approximation is used to determine the scaling factor of a certain mode between two setups. The scaling factor is different from one if the (unknown) excitation changes from one setup to another, which is generally the case. The whole procedure is summarized in Figure 1. For large structures having a huge number of test setups, this approach is time consuming as many stabilization diagrams have to be analyzed. In most of the cases,

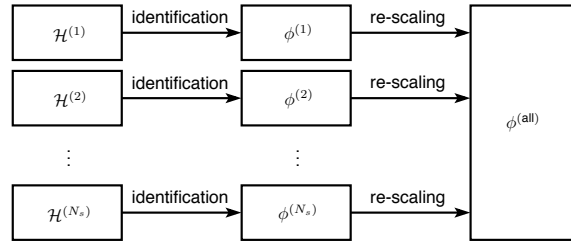


Fig. 1 Merging partial mode shape estimates $\phi^{(j)}$, $j = 1, \dots, N_s$ into a global mode shape estimate $\phi^{(\text{all})}$ in the PoSER approach.

all modes are not well excited in all setups and mode pairing between different setups is difficult.

3.2 Pre Global Estimation Re-Scaling (PreGER)

3.2.1 General PreGER Merging Strategy

The PreGER merging approach was introduced in [9, 10] and recently generalized [6, 8]. It makes use of a factorization of the subspace matrix of each setup into observability and some other matrix on the right side, and normalizes them with a common right factor to introduce the same excitation factor to all the setups. In this work, it is simplified and adapted to a large number of setups.

For each setup $j = 1, \dots, N_s$ the subspace matrix (7) is built that has the factorization property $\mathcal{H}^{(j)} = \mathcal{O}^{(j)} \mathcal{X}^{(j)}$. In order to merge the data, first the different excitation factors of each setup are taken into account, which are present in the Kalman filter state sequence $\mathcal{X}^{(j)}$ since the matrix of observability is only dependent of the observation matrix $H^{(j)}$ and state matrix F that are not affected. In the first step, all the subspace matrices $\mathcal{H}^{(j)}$ are re-scaled with a common Kalman filter state sequence $\mathcal{X}^{(j^*)}$ of one fixed setup j^* , then the resulting matrices are merged and a global modal parameter estimation is finally done on the merged matrix.

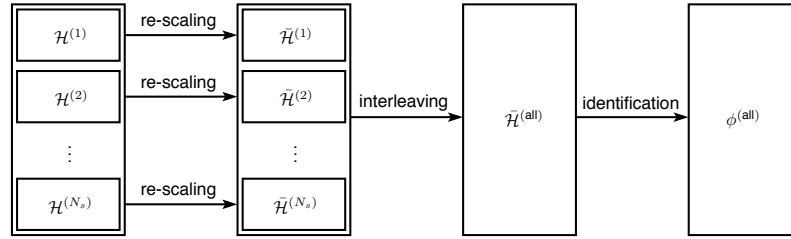


Fig. 2 Merging subspace matrices of each setup to obtain a global subspace matrix and global mode shape estimate $\phi^{(\text{all})}$ in the PreGER approach from [6, 8].

In detail (see also [6]), the subspace matrices $\mathcal{H}^{(j)}$ are separated into matrices $\mathcal{H}^{(j,\text{ref})}$ and $\mathcal{H}^{(j,\text{mov})}$ by taking the appropriate rows of $\mathcal{H}^{(j)}$ that correspond to the reference resp. moving sensor data from $\mathcal{Y}_{(j,\text{ref})}^+$ resp. $\mathcal{Y}_{(j,\text{mov})}^+$. Then, the matrices $\mathcal{H}^{(j,\text{ref})}$, $j = 1, \dots, N_s$ are juxtaposed to

$$\mathcal{H}^{(\text{all},\text{ref})} = (\mathcal{H}^{(1,\text{ref})} \mathcal{H}^{(2,\text{ref})} \dots \mathcal{H}^{(N_s,\text{ref})})$$

and with the help of an SVD this matrix is decomposed to

$$\mathcal{H}^{(\text{all},\text{ref})} = \mathcal{O}^{(\text{ref})} (\mathcal{X}^{(1)} \mathcal{X}^{(2)} \dots \mathcal{X}^{(N_s)}), \quad (8)$$

from where the matrices $\mathcal{X}^{(j)}$ and the observability matrix with respect to the reference sensors $\mathcal{O}^{(\text{ref})}$ are obtained. One of the setups $j^* \in \{1, \dots, N_s\}$ is chosen and the matrices $\mathcal{H}^{(j, \text{mov})}$ are rescaled to

$$\bar{\mathcal{H}}^{(j, \text{mov})} = \mathcal{H}^{(j, \text{mov})} \mathcal{X}^{(j)\dagger} \mathcal{X}^{(j^*)},$$

where \dagger denotes the pseudoinverse. In the last step the block rows of the matrices $\bar{\mathcal{H}}^{(j, \text{mov})}$, $j = 1, \dots, N_s$, and the matrix $\mathcal{H}^{(j^*, \text{ref})}$ are interleaved, to obtain the merged matrix $\bar{\mathcal{H}}^{(\text{all})}$ with the factorization property

$$\bar{\mathcal{H}}^{(\text{all})} = \mathcal{O}^{(\text{all})} \mathcal{X}^{(j^*)} \quad \text{with} \quad \mathcal{O}^{(\text{all})} = \begin{pmatrix} H^{(\text{all})} \\ H^{(\text{all})} F \\ H^{(\text{all})} F^2 \\ \vdots \\ H^{(\text{all})} F^p \end{pmatrix} \quad \text{and} \quad H^{(\text{all})} = \begin{pmatrix} H^{(\text{ref})} \\ H^{(1, \text{mov})} \\ H^{(2, \text{mov})} \\ \vdots \\ H^{(N_s, \text{mov})} \end{pmatrix}. \quad (9)$$

On this global subspace matrix the subspace system identification can be performed to obtain the global modal parameters.

3.2.2 Modular PreGER Merging Strategy

The PreGER approach is now modified to handle a large number of setups, as in such a case the global subspace matrix $\bar{\mathcal{H}}^{(\text{all})}$ can get very big, which can pose memory problems. Also, an SVD of $\bar{\mathcal{H}}^{(\text{all})}$ has to be done to obtain the observability matrix $\mathcal{O}^{(\text{all})}$, and from this matrix the state transition matrix F is obtained from a least squares solution. These are operations involving large matrices in the case of many setups and memory problems can arise again.

In order to circumvent these problems, the matrix $\mathcal{O}^{(\text{all})}$ is built directly instead of $\bar{\mathcal{H}}^{(\text{all})}$, similar to the modular merging approach in [7], so that no further SVD has to be done. With $\mathcal{O}^{(j, \text{mov})} \stackrel{\text{def}}{=} \mathcal{H}^{(j, \text{mov})} \mathcal{X}^{(j)\dagger}$ and Equation (9), $\mathcal{O}^{(\text{all})}$ can also be built directly by interleaving the block rows of the matrices $\mathcal{O}^{(j, \text{mov})}$, $j = 1, \dots, N_s$, and the matrix $\mathcal{O}^{(\text{ref})}$. From $\mathcal{H}^{(j, \text{ref})} = \mathcal{O}^{(\text{ref})} \mathcal{X}^{(j)}$ the relation

$$\mathcal{O}^{(j, \text{mov})} = \mathcal{H}^{(j, \text{mov})} \mathcal{X}^{(j)\dagger} = \mathcal{H}^{(j, \text{mov})} \mathcal{H}^{(j, \text{ref})\dagger} \mathcal{O}^{(\text{ref})}$$

follows and hence in Equation (8) only the matrix $\mathcal{O}^{(\text{ref})}$ is needed. Then, the SSI using the modular PreGER merging – only involving small matrices coming from single setups if necessary – consists of the following steps:

- Get the matrix $\mathcal{O}^{(\text{ref})}$ from the SVD of $(\mathcal{H}^{(1, \text{ref})} \mathcal{H}^{(2, \text{ref})} \dots \mathcal{H}^{(N_s, \text{ref})})$. If the latter matrix is too big, an iterative thin RQ decomposition can be done prior to the SVD, that involves only one matrix $\mathcal{H}^{(j, \text{ref})}$ in one step. See also [7] for details.
- Build the matrices $\mathcal{O}^{(j, \text{mov})} = \mathcal{H}^{(j, \text{mov})} \mathcal{H}^{(j, \text{ref})\dagger} \mathcal{O}^{(\text{ref})}$, $j = 1, \dots, N_s$

- Solve the least squares problem for the state transition matrix F either from $\mathcal{O}^{(\text{all})}$ (which results from interleaving $\mathcal{O}^{(j,\text{mov})}$, $j = 1, \dots, N_s$, and $\mathcal{O}^{(\text{ref})}$) or iteratively by directly using the matrices $\mathcal{O}^{(j,\text{mov})}$, $j = 1, \dots, N_s$, and $\mathcal{O}^{(\text{ref})}$ one after each other, see also [7] for details. Get the global observation matrix $H^{(\text{all})}$ from the first block row of $\mathcal{O}^{(j,\text{mov})}$, $j = 1, \dots, N_s$, and $\mathcal{O}^{(\text{ref})}$.
- Get the natural frequencies, damping ratios and mode shapes from F and $H^{(\text{all})}$.

This modular PreGER approach is summarized in Figure 3.

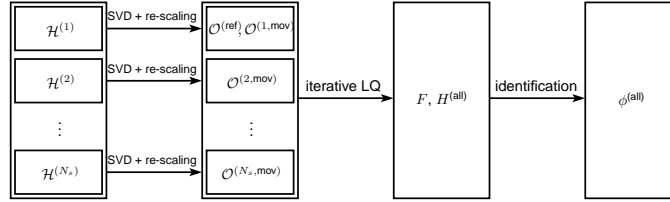


Fig. 3 Merging subspace matrices of each setup to obtain a global subspace matrix and global mode shape estimate $\phi^{(\text{all})}$ in the modular PreGER approach.

4 Analysis of Humber Bridge

4.1 Bridge Description and Ambient Vibration Test

The Humber Bridge (Figure 4), which was opened in July 1981, has a main span of 1410 m with side spans of 280 m and 530 m. The spans comprise 124 units of 18.1 m long 4.5 m deep 140 prefabricated sections 28.5 m wide including two 3 m walkways. The top of the box section constitutes an orthotropic plate on which



Fig. 4 Views of Humber Bridge from North and South.

mastic asphalt surfacing is laid, and the sections have four internal bulkheads. At the end of each span there is a pair of A-frame rocker bearings that provide restraint in three degrees of freedom. The slip-formed reinforced concrete towers rise 155.5 above the caisson foundations and carry the two main cables which have a sag of 115.5 m. These cables each have sectional area of 0.29 m^2 and consist of almost 15,000 5 mm 1.54 kN/mm^2 UTS wires grouped in strands.

The bridge was previously tested in July 1985 [2]. The testing was motivated by a requirement to validate FE procedures for suspensions bridges. The 1985 testing used only three accelerometers, several km of cables, an analog tape recorder and a two-channel spectrum analyzer and it was possible to identify over 100 vibration modes of the main span, side spans and towers up to a frequency of 2 Hz. After 23 years, the original signals and resulting digital mode shapes were no longer available, just the values in published papers and reports. Because of the quality uncertainties and lack of digital data for the EPSRC project, a retest of the bridge was necessary.

The current test was conducted during the week 14th-18th in July 2008 as part of EPSRC funded research project. To avoid lengthy post-processing of data a different strategy was required for the system identification, making use of autonomous recorders with precise timing of GPS-synchronized clocks. The system for using autonomous recorders pioneered by researchers at FEUP in Portugal [4, 5] was adopted and a team from FEUP brought their recorders and assisted in the testing and post-processing. Between FEUP and University of Sheffield ten GEOSIG recorders were available. These recorders used either internal force balance accelerometers, external Guralp CMG5 accelerometers of a triaxial arrangement of QA750 accelerometers.

With up to five days of measurement available with a maximum of 10 hours per day due to recorder batteries, an optimal plan was formulated that involved separate setups to cover 76 positions. Sensor locations for one of the setup is shown in Figure 5, in each of these two pairs of triaxial recorders would be maintained at two permanent reference locations, leaving the remaining three pairs to rove either deck or in East/West tower pylons. Each measurement generated one hour of 30-channel (10 in each direction) acceleration records, in four 15-minute segments. The entire day of measurements was pre-programmed into each recorder, leaving 10-minute periods between measurements to move the six rovers. Several cross-calibration measurements were made to test the synchronization and relative calibrations of the recorders by positioning them together. For side-span measurements an extra pair of recorders was kept as a side-span reference and on the final day, a single pair of recorders was kept in the main span with a pair of recorder left on the top of each



Fig. 5 Sensor locations for setup 24: sidespan measurement.

tower (one on each pylon) and the remaining pairs roved in the tower. The details of test procedure can be found in [3].

4.2 *Preprocessing of the Data*

In this work, only vertical direction data from 26 different setups are processed. The analysis of the experimental data involved initial preprocessing operations of trend removal, low-pass filtering and resampling, considering that the range of frequencies of interest is rather low, of the order of 1 Hz, compared to the original sampling rate of 100 Hz.

4.3 *PoSER Approach*

Several values for SSI parameters are tried and the following parameters are selected:

- Expected system order: 45
- Model order range: 2, 4, 6, 8, . . . , 100
- References: 4 reference channels

The set of 18 modes that had been extracted from the data in the frequency range of interest [0-1 Hz] is shown in Figure 6. These modes can be characterized as:

- Vertical bending modes 1, 3 and 4 possesses symmetry in all three spans.
- Vertical modes 5, 8 and 11 and torsional mode 10 possesses anti-symmetry in main span and symmetry in long side span.
- Vertical modes 6, 9, 12, 15, 18 and torsional mode 13 have symmetry in main span.
- Vertical mode 2 possesses symmetry with respect to sides spans and anti-symmetry in main span.
- Vertical mode 7 possesses symmetry with respect to main span and long side span.
- Vertical modes 14 and 17 and torsional mode 16 possesses anti-symmetry in main span.

The shapes of the 6th vertical mode is not found perfect due to difficulty in analyzing the very closely spaced mode in the stabilization diagram. The extracted modal parameters are in good agreement with other methods that are reported in [3] except the values of the damping ratios.

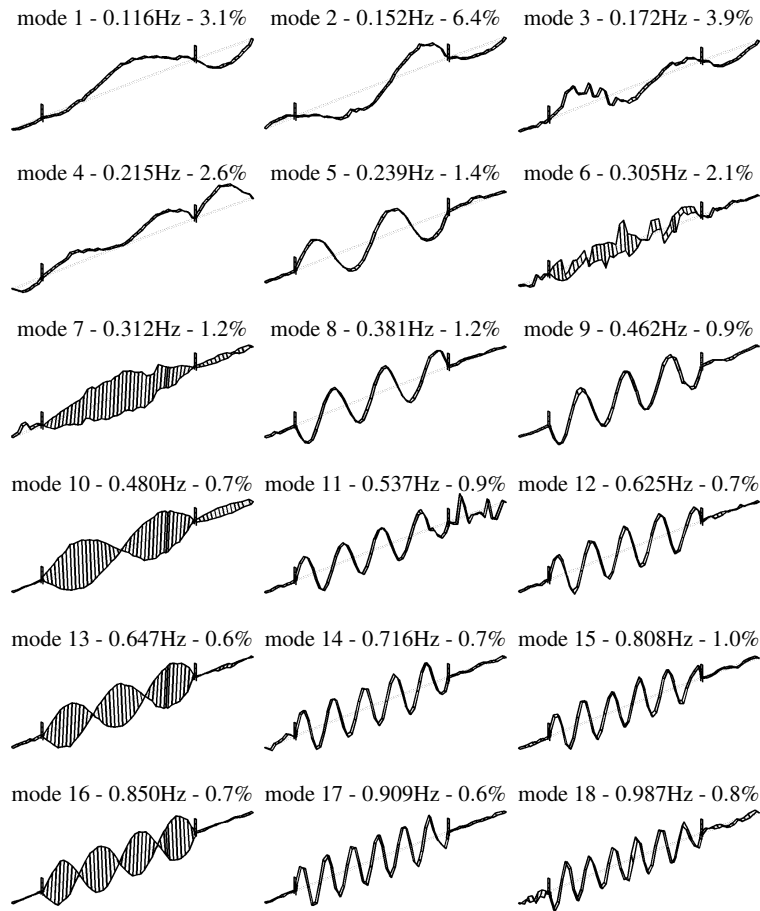


Fig. 6 Modes identified with data-driven SSI from the PoSER approach.

4.4 PreGER Approach

For the PreGER merging approach, all 26 setups were processed together and special care was taken of the presence of the data from the different setups and the resulting partial subspace matrices in memory only when they were needed for the merging procedure described in Section 3.2.2. For the analysis $p + 1 = q = 50$ was selected to build the subspace matrices, and having 4 reference sensors available the maximal model order was 200. The stabilization diagram obtained from the global merged subspace matrix is presented in Figure 8, from where the modes were chosen.

All the identified mode shapes can be seen in Figure 7. They correspond very well to the results of the PoSER approach, as well as the frequencies and damping ratios. However, the very closely spaced modes 6 and 7 are well separated now.

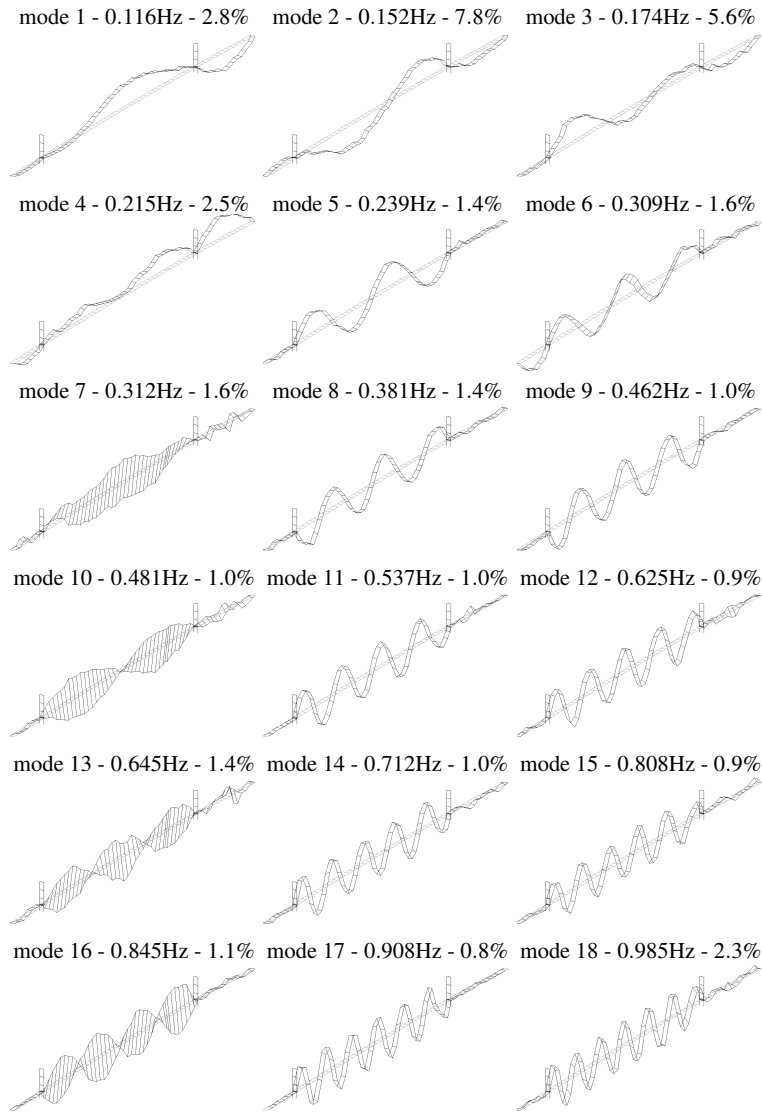


Fig. 7 Modes identified with data-driven SSI from the modular PreGER approach.

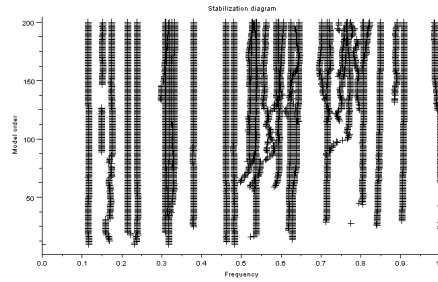


Fig. 8 Stabilization diagram containing the natural frequencies of Humber bridge from the PreGER approach.

5 Summary of Results and Comparison

Table 1 provides a comparative overview of the natural frequencies and damping ratios estimated with the PoSER and PreGER merging approach using the data-driven SSI-cov/ref method. For a comparison of the mode shapes the Modal Assurance Criterion (MAC) of the real parts of the mode shapes between PoSER and PreGER approach is shown in Figure 9. The following observations can be made:

#	PoSER		PreGER	
	f (in Hz)	d (in %)	f (in Hz)	d (in %)
1	0.116	3.1	0.116	2.8
2	0.152	6.4	0.152	7.8
3	0.172	3.9	0.174	5.6
4	0.215	2.6	0.215	2.5
5	0.239	1.4	0.239	1.4
6	0.305	2.1	0.309	1.6
7	0.312	1.2	0.312	1.6
8	0.381	1.2	0.381	1.4
9	0.462	0.9	0.462	1.0
10	0.480	0.7	0.481	1.0
11	0.537	0.9	0.537	1.0
12	0.625	0.7	0.625	0.9
13	0.647	0.6	0.645	1.4
14	0.716	0.7	0.712	1.0
15	0.808	1.0	0.808	0.9
16	0.850	0.7	0.845	1.1
17	0.909	0.6	0.908	0.8
18	0.987	0.8	0.985	2.3

Table 1 An overview of the estimated natural frequencies f and damping ratios d obtained from the different merging strategies using data-driven SSI.

- The differences in natural frequencies for the PoSER and the PreGER approach are less than 1 %.
- For the damping ratios, the differences between PoSER and PreGER estimates are larger but still not significant considering the large standard deviations on the estimates. In general, the PreGER estimates are slightly larger than the PoSER estimate, which might be due to the fact, that the natural frequencies in each setup are slightly different. Then, the resulting frequency for each mode obtained by the PreGER approach is associated to a higher damping ratio, consequence from the merging of overlapping frequencies.
- The MAC values between most of the mode shapes of the different merging approaches are very close to one, meaning that the identified mode shapes are very similar. Only mode shape 6, that could not be identified clearly in the PoSER approach, shows a big difference. Also mode shape 11 shows some difference, due to some noise in the mode shape estimate of the PoSER approach in the side span of the bridge, that is not present in the PreGER approach.

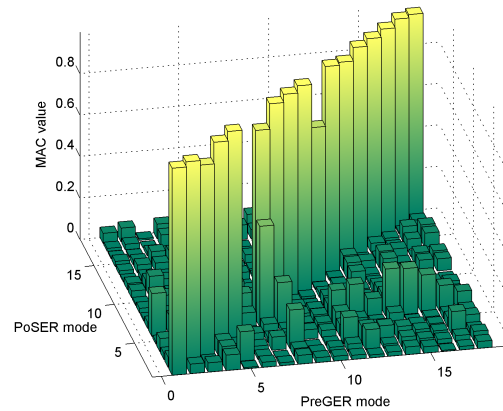


Fig. 9 MAC values between the real parts of the mode shapes obtained by PoSER and PreGER approach.

6 Conclusion

In this work, the PreGER merging approach for Stochastic Subspace Identification was further modified to handle a large number of measurement setups containing moving sensors and a set of fixed reference sensors. It is adapted to be completely modular and hence it has the same memory requirements as the PoSER merging approach.

Both PoSER and PreGER approaches offer comparable qualitative modal identification results on the Humber bridge, whereas the PreGER approach has the advantage of also separating closely spaced modes properly. The modal identification results compare well with previously published results from different identification algorithms in [3], showing also the feasibility of the new PreGER merging approach. In addition, the PreGER merging approach may have the following preferences:

- theoretically sound, taking the difference in the excitation already in the modeling into account;
- just one stabilization diagram has to be analyzed without the need of matching of modes between measurement setups.

Acknowledgments

This work was partially supported by the European project FP7-NMP CP-IP 213968-2 IRIS.

References

1. Basseville, M., Benveniste, A., Goursat, M., Hermans, L., Mevel, L., van der Auweraer, H.: Output-only subspace-based structural identification: from theory to industrial testing practice. *Journal of Dynamic Systems, Measurement, and Control* **123**(4), 668–676 (2001)
2. Brownjohn, J., Dumanoglu, A., Severn, R., Taylor, C.: Ambient vibration measurements of the humber suspension bridge and comparison with calculated characteristics. In: *Proc. of the Institution of Civil Engineers (London)*, vol. 83, pp. 561–600 (1987)
3. Brownjohn, J., Magalhães, F., Caetano, E., Cunha, A.: Ambient vibration re-testing and operational modal analysis of the Humber Bridge. *Engineering Structures* **32**(8), 2003–2018 (2010)
4. Cunha, A., Caetano, E., Delgado, R.: Dynamic tests on large cable-stayed bridge. *Journal of Bridge Engineering* **6**(1), 54–62 (2001)
5. Cunha, A., Caetano, E., Magalhães, F.: Output-only dynamic testing of bridges and special structures. *Structural Concrete* **8**(2), 67–86 (2007)
6. Döhler, M., Andersen, P., Mevel, L.: Data merging for multi-setup operational modal analysis with data-driven SSI. In: *Proceedings of the 28th International Modal Analysis Conference (IMAC-XXVIII)*. Jacksonville, FL, USA (2010)
7. Döhler, M., Mevel, L.: Modular subspace-based system identification and damage detection on large structures. In: *Proceedings of the 34th IABSE Symposium*. Venice, Italy (2010)
8. Döhler, M., Reynders, E., Magalhães, F., Mevel, L., Roeck, G.D., Cunha, A.: Pre- and post-identification merging for multi-setup OMA with covariance-driven SSI. In: *Proceedings of the 28th International Modal Analysis Conference (IMAC-XXVIII)*. Jacksonville, FL, USA (2010)
9. Mevel, L., Basseville, M., Benveniste, A., Goursat, M.: Merging sensor data from multiple measurement setups for nonstationary subspace-based modal analysis. *Journal of Sound and Vibration* **249**(4), 719–741 (2002)
10. Mevel, L., Benveniste, A., Basseville, M., Goursat, M.: Blind subspace-based eigenstructure identification under nonstationary excitation using moving sensors. *IEEE Transactions on Signal Processing* **SP-50**(1), 41–48 (2002)

11. van Overschee, P., De Moor, B.: Subspace Identification for Linear Systems: Theory, Implementation, Applications. Kluwer (1996)
12. Peeters, B., De Roeck, G.: Reference-based stochastic subspace identification for output-only modal analysis. *Mechanical Systems and Signal Processing* **13**(6), 855–878 (1999)